STABILITY ANALYSIS OF STATIC SLIP-ENERGY RECOVERY DRIVE VIA EIGENVALUE METHOD

*OTI S. EJIOFOR and **O.I. OKORO
Department of Electrical Engineering,
University of Nigeria, Nsukka.
Enugu State.

*Email: otisteveofor@yahoo.com **Email: oiokoro@hotmail.com

ABSTRACT

The stability of the sub synchronous static slip energy recovery scheme for the speed control of slip-ring induction motor is presented. A set of nonlinear differential equations which describe the system dynamics are derived and linearized about an operating point using perturbation technique. The Eigenvalue analysis of the linearized model shows that the drive system is almost completely stable in the entire operating range Routh stability criterion is used in the polar plots of roots of the characteristics equations of induction machine drive on the σ-jω plane which further justified the above results.

Key words: Stability, Eigenvalue, Firing angle, Polar plots

LIST OF SYMBOLS

α Firing angle of the inverter

H Inertia constant

R_s Stator winding resistance

R_r Rotor winding resistance to the stator

X_r Rotor reactance at base frequency referred to stator

X_s stator reactance at base frequency

i_{ds}, i_{qs} D-q stator current

i_{dr}, i_{qr} Referred rotor d-q currents

T_e Electromagnetic torque developed

T_l load torque

X_f filter reactance at base frequency referred to stator

R_f filter resistance at base frequency referred to stator

L_f filter inductance

S Motor slip

V_s stator phase voltage

X_m mutual reactance at base frequency

V_r Rotor phase voltage in the synchronous frame

ω_r Rotor electrical angular frequency in radians per second

ω, ω_b base electrical angular frequency in radians per second

V_{sm} peak value of phase voltage on the a.c side of inverter

V_{rm} peaks value of V'_r

I_D Rectifier output current

V_D Rectifier output voltage

V_{op} Counter Emf of the inverter

Subscript 'o' Indicates the steady state variables

1. 0 INTRODUCTION

The DC, synchronous and induction machines are the major work tools in the industries with the later dominating in application. In more comparative terms, the squirrel cage induction motor is lighter, more robust, and less expensive, has higher torque-inertia ratio and is capable of much higher speed [1]. Its output power is also much higher. However, its speed control is more complex with the result that the conventional methods of the speed control have been either expensive or highly inefficient. There are complexities in modeling induction motors owing to the many non linearities of the parameters. With the recent development and progress in power semiconductor technology, the undesirable features of the conventional rheostatic control schemes can be eliminated by using a three phase rectifier bridge connected to the slip rings. The system is supplied via a D.C reactor and a chopper which are connected in parallel with the disadvantages of producing high losses due to slip power dissipation.

The popularity of this drive stems from the fact that the slip power is recovered in the rectifier-inverter media and returned to the supply giving rise to a constant torque drive. This scheme provides a viable variable speed drive with the inverter firing angle as the speed-control parameter when the direct feedback of current is in progress.

In the study of the systems stability, Mittle et al [2] determined the instability region using the characteristic equation of the linearized model obtained from the motional impedance matrix of the system. This was done by the application of the Routh-Hurwitz criterion to the characteristic equation.

Subrahmanyan et al [3] stated that there exist numerical errors associated with the determination of the coefficient of the equations and thereof the discrepancy between the result of [3] and those of Mittle et al. In the work presented by Subrahmanyam, the small signal perturbation method and eigenvalue analysis were adopted in the study of the system stability. In the work, the stability of the system at any operating point is determined by the eigenvalues of the particular matrix formed from the linearized equations of the system.

Reports by many authors [2] indicate that the inverter-fed induction motor drives exhibit instability at lower speeds of operation. Mittle et al confirmed the presence of instability regions which according to [2] are present at low values of moments of inertia, and increase substantially with an increase in applied voltage.

However, in a sharp contrast, [3] has it that the above drive is stable throughout the operating range as far as normal operation is concerned. Subrahmanyam et al added that concerning the transient analysis of the system, that at all those points, the system reached the new steady state within a reasonable time.

In the light of the above contradictory propositions and arguments, there is need for a clearer study of the dynamics and stability of the drive. The Eigenvalues analysis of the linearized model of an induction motor by the small signal perturbation method shows that the system in general terms does not become unstable.

2.0 Simulation Parameters: The parameters of the machine studied are summarized in table 1 below.

Table 1: Simulation parameters

Slip-Ring Induction Motor (PER UNIT PARAMETERS)	VALUES
Motor rated power	5-hp
Inertia constant, H	0.25s
Rated voltage, V	400 V
Base frequency, ω_b	60Hz
Type of connection	Star connected
Filter parameters (p.u)	
Filter reactance, X'_f	1.0
Filter resistance, R'_f	0.02

Ohmic parameters (p.u)	
Stator resistance, R_s	0.058
Stator leakage reactance ,X_s	3.0
Rotor winding resistance, R'_r	0.072
Magnetizing reactance, X_m	2.9
Rotor reactance, X'_r	3.0

3.0 EQUATIONS OF THE SYSTEM

The equations which describe the symmetrical three phase induction machine in a synchronously rotating reference frame as given by [5] can be written in per unit as in [2,3].

$$\begin{bmatrix} V_{ds} \\ V_{qs} \\ V_{dr} \\ V_{qr} \end{bmatrix} = \begin{bmatrix} R_s + X_s(P/\omega) & -\times_s & -\times_m (p/\omega) & -\times_m \\ \times_s & R_s + \times_s (P/\omega) & \times_m & \times_m (p/\omega) \\ \times_m (P/\omega) & -sX_m & R_r + X_r(P/\omega) & -sX_r \\ sX_m & \times_m (P/\omega) & sX_r & R_r + \times_r (P/\omega) \end{bmatrix} \begin{bmatrix} i_{ds} \\ i_{qs} \\ i_{dr} \\ i_{qr} \end{bmatrix} \quad (1)$$

$$\text{where } p = \frac{d}{dt} \quad (2)$$

$$s = \frac{\omega - \omega_r}{\omega} \quad (3)$$

$\omega = \omega_b$ angular frequency and = the electrical speed of the rotor. The electromagnetic torque developed in per unit is given by;

$$T_e = \times_m (i_{qs} i_{dr} - i_{ds} i_{qr}) \quad (4)$$

In deriving the equations for the stability studies of a slip energy recovery scheme, the following assumptions are made:

(i) the induction motor is ideal and symmetric
(ii) the switching elements are ideal
(iii) the rectifier output is continuous
(iv) the commutation of the rectifier and the inverter are instantaneous
(v) higher harmonics in the rectifier output have negligible effect on the stability.

Having assumed as above and neglecting the effects of harmonics and commutation, the average output voltage of a three-phase full-wave uncontrolled rectifier bridge is;

$$V_D = \frac{3\sqrt{3}}{\pi} V_{rm} \quad (5)$$

where V_{rm} is the peak value of the rotor phase voltage at the slip ring of the induction motor. If the a.c source impedance is ignored and the voltage assumed infinitely smoothed then, the opposing electromotive force (E.M.F) of the inverter which is a function of the firing angle and supply voltage will be given by;

$$V_{op} = \frac{3\sqrt{3}}{\pi} V_{rm} \cos(\pi - \alpha) \quad (6)$$

Where α is the inverter firing angle and is the maximum value of the phase voltage on the a.c. side of the inverter. Since at time (t = 0) the q-axis of the synchronous rotating reference frame coincides with the magnetic axis of the stator reference frame, the quadrature component of the supply voltage V_{qs} will be equal to the peak value of line to neutral voltage V_{sm} and the direct component V_{ds} zero, therefore equation (6) becomes;

$$V_{op} = \frac{3\sqrt{3}}{\pi} V_{qs} \cos(\pi - \alpha) \qquad (7)$$

Continuous conduction assumption means that the voltage equation for the filter can be written as;

$$V_D = V_{op} + ((R_f + X(p/\omega))i_D \qquad (8)$$

Also if the angular, that is the phase relationship between the q-axis and the magnetic axis of the stator and the rotor phases is selected so that they coincide at time t = 0, the q-axis voltages of the stator and the rotor will be zero. The q-axis voltage will be equal to the peak value of the respective phase voltages, that is,

$$V_{ds} = 0 \qquad (9)$$

$$V_{qs} = V_{sm} \qquad (10)$$

$$V'_{dr} = 0 \qquad (11)$$

$$V'_{qr} = V_{rm} \qquad (12)$$

$$\therefore V'_{qr} = V_{rm} = \left(\pi/3\sqrt{3}\right)V_D \qquad (13)$$

An approximate relation between the direct link current I_D and the q-axis rotor current i_{qr} can be obtained by equating the input and output power of the rectifier and neglecting losses, that is;

$$V_D I_D = -1.5V'_{qr}i'_{qr} \qquad (14)$$

where i'_{qr} is the quadrature component of current fed to the rectifier. An input power to the rotor is considered, that is why there is negative sign in equation (14) we get the direct link current,

$$I_D = -0.906[i_{qr}] \qquad (15)$$

Combining equations (5), (8), (12) and (15) above we get;

$$V'_{qr} = -V_{sm}\cos\alpha + (\pi^2/18)\left(R'_f + \times'_f(p/\omega)\right) i'_{qr} \qquad (16)$$

Equations (4) to (14) together with equation (I) describe the dynamics of the static slip energy -recovery drive. When equations (9) - (II) and (16) are substituted in equation (I) the resulting matrix equation of the drive becomes;

$$\begin{bmatrix} 0 \\ V_{sm} \\ 0 \\ -V_{sm}\cos\alpha \end{bmatrix} = \begin{bmatrix} R_s + X_s(P/\omega) & -\times_s & -\times_m(P/\omega) & -\times_m \\ \times_s & R_s + \times_s(P/\omega) & \times_m & \times_m(P/\omega) \\ \times_m(P/\omega) & -s_o X_m & F + X'_r(P/\omega) & -sX'_r \\ s_O X_m \quad \times_m(P/\omega) & s_O X'_r & & R'_r + \times'_r(P/\omega) + \pi^2\left(R'_f + \times'_f(P/\omega)\right)/18 \end{bmatrix} \begin{bmatrix} i_{ds} \\ i_{qs} \\ i'_{dr} \\ i'_{qr} \end{bmatrix}$$

Where the electromagnetic behaviour of the system is given as

$$T_e - T_l = 2\omega H(P/\omega)(\omega_r/\omega) \qquad (18)$$

And (ω_r/ω) is the per angular speed of the rotor. The overall behaviour of the system is fully described by equation (4), (17) and (18).

The digital simulation of the system is enhanced by presenting the above equations in state variable form as shown below with currents as state as state variables:

$$(P/\omega_b)i_{ds} = -\frac{R_s X'_r}{K} i_{ds} + \frac{(X_s X'_r - X_m^2)}{K} i_{qs} + \frac{X_m R'_r}{K} i'_{dr} + \frac{(1-s_o) X_m X_r}{K} i_{qr} \quad (19)$$

$$(P/\omega_b)i_{qs} = \frac{V_{sm}(X_m \cos\alpha + X_{rf})}{W} - \frac{(X_{rf} X_s - s_o X_m^2)}{W} i_{ds} - \frac{X_{rf} R_s}{W} i_{qs} - \frac{(X_{rf} - s_o X'_r) X_m i'_{dr}}{W} + \frac{R_{rf} X_m}{W} i'_{qr} \quad \ldots\ldots (20)$$

$$(P/\omega_b)i'_{dr} = -\frac{(1-s_o) X_m X_s}{K} i_{qs} - \frac{(X_s R'_r)}{K} i'_{dr} + \frac{(s_o X_s X'_r - X_m^2)}{K} i'_{qr} + \frac{R_s X_m}{k} i_{ds} \quad (21)$$

$$(P/\omega_b)i'_{qr} = -\frac{V_{sm}(X_s \cos\alpha + X_m)}{W} + \frac{(1-s_o) X_m X_s}{W} i_{ds} + \frac{X_m R_s}{W} i_{qs} - \frac{(s_o X_s X'_r - X_m^2) i'_{dr}}{W} - \frac{X_m R_{rf}}{W} i'_{qr} \quad (22)$$

$$(P/\omega_b)\left(\frac{\omega_r}{\omega_b}\right) = \left[\frac{1}{\omega_b H}\right]\left(X_m\left(i_{qs} i'_{dr} - i_{ds} i'_{qs}\right) - T_l\right) \quad (23)$$

Where,

$$s - 1 = \frac{\omega_r}{\omega_b} \quad (24)$$

$$K = X_s X'_r - X_m^2 \quad (25)$$

$$W = X_{rf} X_s - X_m^2 \quad (26)$$

$$X_{rf} = X'_r + (\pi^2/18) X'_f \quad (27)$$

$$R_{rf} = R'_r + (\pi^2/18) R'_f \quad (28)$$

The above equations having all the variables in equations (17) and (18) except V_{sm} and ά changed by small amount about a steady operating point would, if the steady- state terms are eliminated and the higher order incremental terms neglected, give a linearized small displacement equation written in the form,

$$\dot{X} = AX + Bu \quad (29)$$

$$\left(\frac{P}{\omega_b}\right)\begin{bmatrix} i_{ds} \\ i_{qs} \\ i'_{dr} \\ i'_{qr} \\ \omega_r/\omega_b \end{bmatrix} = A \begin{bmatrix} i_{ds} \\ i_{qs} \\ i'_{dr} \\ i'_{qr} \\ \omega_r/\omega_b \end{bmatrix} + \begin{bmatrix} 0 \\ 0 \\ 0 \\ 0 \\ -T_1/2\omega_b H \end{bmatrix} \quad (30)$$

Where the system matrix A for ease of simulation is presented as shown;

$$\begin{bmatrix} -\frac{R_s X'_r}{K} & \frac{(X_s X'_r - s_o X_m^2)}{K} & \frac{X_m R'_r}{K} & \frac{(1-so) X_m X'_r}{K} & \frac{X_m G}{K} \\ \frac{s_o X_m^2 - X_s X_{rf}}{W} & -\frac{R_s X_{rf}}{W} & \frac{(-(1-s_o) X_m X'_r - \pi^2 X_m X'_f/18)}{W} & \frac{X_m R_{rf}}{W} & -\frac{X_m F}{w} \\ \frac{R_s X_m}{K} & -\frac{(1-s_o) X_m X_s}{K} & -\frac{X_s R'_r}{K} & \frac{(s_o X_s X'_r - X_m^2)}{K} & -\frac{X_s G}{K} \\ \frac{(1-s_o) X_m X_S}{W} & \frac{X_m R_s}{W} & \frac{X_m^2 - s_o X_s X'_r}{W} & -\frac{X_s R_{rf}}{W} & \frac{X_s F}{W} \\ -\frac{X_m}{2\omega_b H} i'_{qro} & \frac{X_m}{2\omega_b H} i'_{dro} & \frac{X_m}{2\omega_b H} i_{qso} & -\frac{X_m}{2\omega_b H} i_{dso} & 0 \end{bmatrix} \quad \ldots(31)$$

Where,

$$G = \frac{(X_m i_{qso} + X_m i'_{qro})}{\omega} \quad (32)$$

$$F = \frac{(X_m i_{qso} + X_m i'_{qro})}{\omega} \quad (33)$$

$$K = X_s X'_r - X_m^2 \quad (34)$$

$$H = X_s X'_r - s_O X_m^2 + 0.55 X'_f X_s \quad (35)$$

The study of the stability of the system in the entire operating region is therefore realized by determining the eigenvalues of system matrix of equation (31) at, different values of slip from the least to the highest values which correspond to various fixed values of the firing angle, alpha, which in this case is from 90 degrees to 170 degrees. This is carried out using Matlab [6]. Now, if all the eigenvalues have negative real parts then the system is stable while if any of the eigenvalues has positive real part, then the system at that point is unstable.

4.0 RESULTS

The results obtained from the program simulation for the operating range are presented in tabular from as shown below.

DETERMINATION OF THE EIGENVALUES FOR A GIVEN FIRING ANGLE (ALPHA) AT DIFFERENT OPERATING POINTS [increasing left to right].

-0.0859+09573i -0.0859-09573i -02709+02570i -0.2709-02570i -0.1510	-0.0744+09613i -0.0744-0963i -02433+02443i -0.2433-02443i -0.2291	-0.0617+09660i -0.0617-09660i -0.2275+02531i -0.2275-02531i -02861	-0.0478+09717i -0.0478-09717i- 02306+02693i -0.2306-02693i -03076
-0.0859+09788i -0.0328-09788i -02478+02881i -0.2478-02881i -0.3034	-0.0169+09875i -0.0169-09875i -0.2744+03106i -0.2744-03106i -0.2820	-0.0004+09981i -0.0004-09982i -0.3054+03382i -0.3054-03382i -0.2530	0.0163+1.0108i 0.0163-1.0108i -0.3363+03693i -0.3363-03693i -0.2245
-0.0329+1.0257i -0.329-1.025i -0.3653+04257i -0.3653-0.4019i -0.1996	0.0488+1.0427i 0.0488-1.0427i -0.3917+0.4342i -0.33917-0.44342i -0.1787	0.0639+1.0617i 0.0639-1.0617i -0.4156+0.4657i -0.4156-0.4657i -0.1612	**Table 2** **ALPHA = 90 degrees** **SLIP = 0:0.1:.0**

-0.1239+0.9486i -0.1239-0.9486i -0.2096+0.1785i -0.2096-0.1785i -0.1973	-01120+0.9512i -0.1120-0.9512i -0.3056 -0.1675+0.1954i -0.1675-0.1954i	-0.0987+0.9542i -0.0987-0.9542i -0.3392 -0.1639+02172i -0.1639-03172i	-0.841+0.9581i -0.0841-0.9581i -0.1786+02353i -0.1786-02353i -0.3392
-0.0680+0.9486i -0.0680-0.9632i -02080+02632i -02080-02535i -03124	-0.0508+0.9700i -0.0508-0.9700i -0.2490+02790i -0.490-0.2790i -0.2648	-0.0326+0.9789i -0.0326-0.9789i -02913+0.3151i -0.2167	-0.0139+0.9902i -0.0139-0.9902i -03284+0.3550i -0.3284-03550i -0.1800
0.0048+1.0042i 0.0048-1.0042i -0.3606+0.3942i -0.3606-0.3942i -0.1529	0.0229+1.0206i 0.0229-1.0206i -0.3892+0.4312i -03892-0.4312i -0.1320	0.0401+1.0394i 0.0401-1.0394i -0.4147+0.4658i -0.4147-0.4658i -0.1152	**Table 3** **ALPHA = 100 degrees** **SLIP = 0:0.1:1.0**

-0.1516+0.9456i -0.1516-0.9456i -0.3110 -0.1251+0.1305i -0.1251-0.1305i	-0.1396+0.947i -01396-0.9470i -0.3614 -0.1119+0.1654i -0.1119-0.1654i	-0.1264+0.9487i -0.1264-0.9487i -0.3736 -0.1190+0.1861i -0.1190-1861i	-0.1117+0.9511i -0.1117-0.9511i -0.3596 -0.1407+0.2009i -0.1407-0.2009i
-0.0955+0.945i -0.0955-0.9545i -0.3129 -0.1803+02143i -0.18803-02143i	-0.0778+0.9595i -0.0778-0.9595i -0.2388+02437i -0.2388-0.2437i -0.2314	-0.0588+0.9666i -0.0588-0.9666i -0.2886+2934i -0.2886-0.2934i -0.1697	-0.0389+0.9763i -0.0389-0.9763i -0.3266+03427i -0.3266-0327i -0.1335
-0.0187+0.9889i -0.0187-0.9889i -0.3590+0.3878i -0.3590-0.3878i -0.1091	0.0011+1.0044i 0.0011-1.0044i -0.3878+0.4287i -0.3878-0.4287i -0.0910	0.0199+1.-0226i 0.0199-1.0226i -0.4137+0.4659i -0.4137-0.4659i -0.0767	**Table 4** **ALPHA = 110 degrees** **SLIP = 0:0.1:1.0**

-0.1692 + 0.9447i -0.1692-0.9447i -0.3622 -0.0819 + 0.1104i -0.0819 - 0.1104i	-0.1574 + 0.945[illegible]i -0.1574 - 0.9454i -0.3889 -0.0804 +0.1394i -0.0804 - 0.1394i	-0.1444 +0.9463i -0.1444 -0.9463i -0.3[illegible]07 -0.0925 + 0.1565i -0.0925 - 0.1565i	-0.1300 + 0.9477i -0.1300 - 0.9477i -0.3674 -0.1185 + 0.1664i -0.1185 - 0.1664i
-0.1140 + 0.9501i -0.1140 - 0.9501i -0.2992 -0.1686 + 0.3837i -0.1686 - 0.3837i	-0.0964 +0.9538i -0.0964 - 0.9538i -0.2486 + 0.9538i -0.2486 - 0.9538i -0.1743	-0.0773 + 0.9595i -0.0773 - 0.9595i -0.2948 + 02795i -0.2948 - 02795i -0.1203	-0.570 + 0.9678i -0.570 - 0.9678i -0.3291+ 0.3350i -0.3291- 0.3350i -0.0921
-0.362 + 0.9791i -0.362 - 0.9791i -0.3594 + 03837i -0.3594 - 03837i -0.0732	-0.0155 + 0.9935i -0.0155 - 0.9935i -0.3872 + 0.4270i -0.3872 - 0.4270i -0.0591	-0.0044 + 1.019i -0.0044 - 1.019i -0.4126 +04660i -0.4126 -04660i -0.0479	**Table 5** **ALPHA = 120 degrees** **SLIP = 0:0.1:1.0**

-0.1786 +0.9441i -0.1786 - 0.9441i -0.3847 -0.0613 + [illegible]i -0.0613 - [illegible]i	0.1670 + 0.944i 0.1670 - 0.944i -0.4010i -0.0648 + 0.1168i -0.0648 – 0.1168	-0.1542 + 0.9450i -0.1542 - 0.9450i -0.3960 -0.1099 + 0.1321i -0.1099 - 0.1321i	-0.1401 +0.9460i -0.1401 -0.9460i -0.3643 -0.1099 +0.1321i -0.1099 -0.1321i
-0.1246 +0.9478i -0.1246 -0.9478i -0.2524 -0.1815 + 0.12[illegible]4i -0.1815 - 0.1214i	-0.1073 +0.9508i -0.1073 - 0.9508i -0.2684 + 02058i -0.2684 - 02058i -.1131	-0.0885 + 0.9667i -0.0885 - 0.9667i -0.3037 + 02746i -0.3037 - 02746i -0.0801	-0.0683 +0.9630i -0.0683 -0.9630i -0.3334 + 0.3317i -0.3334 - 0.3317i -0.0610
-0.0474 + 0.9733i -0.0474 - 0.9733i -0.3610 + 3818i -0.3610 - 3818i -0.0476	-0.0265 +0.9868i -0.0265 -0.9868i -0.0265 +0.9868i -0.0265 -0.9868i -0.0374	-0.0062 + 1.0034i -0.0062 - 1.0034i -0.4115 +0.4662i -0.4115 -0.4662i -0.0292	**Table 6** **ALPHA = 130 dgrees** **SLIP = 0:0.1:1.0**

-0.1822 + 0.9433i -0.1822 - 0.9433i -0.3939 -0.0531 + 0.0839i -0.531 - 0.0839i	-0.1706 + 0.9435i -0.1506 - 0.9435i -0.4037 -0.0598 + 0.0989i -0.0598 - 0.0989i	-0.1580 + 0.9440i -0.1580 - 0.9440i -0.3932 -0.0776 + 0.1044i -0.0776 - 0.1044i	-0.1442 + 0.9449i -0.1442 - 0.9449i -0.3513 -0.1124 + 0.0962i -0.1124 – 0.0962i
-0.1290 + 0.9465i -0.1290 - 0.9465i -0.2456 + 0.1146i -0.2456 - 0.1146i -0.1153	-0.1121 + 0.9493i -0.1121 - 0.9493i -0.2840 + 0.2093i -0.2840 - 0.2093i -0.0722	-0.0937 + 0.9539i -0.0937 -0.9539i -0.3118 + 02754i -0.3118 - 0.2754i -0.0533	-0.0740 + 0.9607i -0.0740 - 0.9607i -0.3378 + 0.3317i -0.3378 - 0.3317i -0.0410
-0.0534 + 0.9704i -0.0534 - 0.9704i -0.3629 +0.3815i -0.3629 - 0.3815i -0.0319	-0.0326 + 0.9832i -0.0.326 - 0.9832i -0.3872 + 0.4262i -0.3872 - 0.4262i -0.0248	-0.0124 + 0.9992i -0.0124 -0.9992i -0.4103 + 0.4663i -0.4103 - 0.4663i -0.0191	**Table 7** **ALPHA = 140 degrees** **SLIP = 0:0.1:1.0**

-0.1820 + 0.9423i -0.1820 - 0.9423i -0.3958 -0.0523 + 0.0800i -0.0523 - 0.0800i	-0.1705 + 0.9427i -0.1705 - 0.9427i -0.4009 -0.0613 + 0.0859i -0.0613 - 0.0859i	-0.1580 + 0.9432i -01580 - 0.9432i -0.3850 -0.0.817 + 0.0825i -0.0817 - 0.0825i	-0.1444 + 0.9442i -0.1444 - 0.9442i -0.3277 -01240 + 0.0481i -01240 - 0.0481i
-0.1294 + 0.9459i -01294 - 0.9459i -0.2683 + 0.1371i -0.2683 - 0.1371i -0.0690	-0.1129 + 0.9487i -0.1129 - 0.9487i -0.2946 + 0.2165i -0.2946 - 02165i -0.0494	-0.0950 + 0.9532i -0.0950 - 0.9532i -0.03183+ 02788i -0.3183 - 02788i -0.0379	-0.0757 + 0.9598i -0.0757 - 0.99598i -0.3416 + 0.333i -0.3416 - 0.333i -0.0298
-0.0555 + 0.9692i -0.0555 - 0.9692i -0.3648 + 0.3823i -0.3648 - 0.3823i -0.238	-0.0352 + 09817i -0.0352 - 0.9817i -0.3875 +0.4265i -0.3875 - 0.4265i -0.0191	-0.0153 + 0.9972i -0.0153 - 0.9972i -0.4093 + 0.4665i -0.4093 - 0.4665i -0.0153	**Table 8** **ALPHA = 150 degrees** **SLIP = 0:0.1:1.0**

-0.1802 + 0.9414i -0.1802- 0.9414i -0.3941 -0.0550 + 0.800i -0.0550 - 0.800i	-0.1687 + 0.9419i -0.1687-0.9419i -0.3956 -0.0658 + 0.0774i -0.0.658 - 0.0774i	-0.1562 + 0.9426i -0.1562 - 0.9426i -0.3744 -0.0888 + 0.0627i -0.888 - 0.0627i	-0.1427 + 0.9438i -0.1427 - 0.9438i -0.2822 -0.2206 -0.0763
-0.1279 + 0.9456i -0.1279 - 0.9456i -0.2794 + 0.1524i -0.2794 - 0.1524i -0.0498	-0.1117 + 0.9486i -0.1117 - 0.9486i -0.3017 +0.2234i -0.3017 -0.2234i -0.0376	-0.0941 + 0.9531i -0.0941 - 0.9531i -0.3231 + 0.2826i -0.3231 - 0.2826i -0.0300	-0.0753 +0.9598i -0.0753 -0.9598i -0.3446 + 0.334i -0.3446 - 0.334i -0.0246
-0.0556 +0.9690i -0.0556 -0.9690i -0.3663 +0.3833i -0.3663 -0.3833i -0.0206	-0.0357 + 0.9813i -0.0357 - 0.9813i -0.3878 + 0.4269i -0.3878 - 0.4269i -0.0176	-0.0161 +0.9965i -0.0161 - 0.9965i -0.4085 + 0.4667i -0.4085 + 0.4667i -0.0151	**Table 9** **ALPHA = 160 degrees** **SLIP = 0:0.1:1.0**

-0.1783+0948i -0-1783.0948ı -0.3917 -0.0581+0.0811i -0.0581-0.0811i	-0.1668+0941i -0.1668-0941i -0.3907 -0.0701+0.073i -0.0701-0.073i	-0.1544+09423i -0.1544-09423i -03653 -0.0952+0.0460i -0.0952-0.0460i	-0.1410+09435i -0.1410-09435i -0.2617+0.0583i -0.2617 -0.0583i -0.0591
-0.i263+09455i -0.126-09455i -0.2852+0.1617i -02852-0.1617i -0.0415	-01103+09486i -01103-09486i -03058+02283i -03058-02283i -0.0323	-0.0929+0.9532i -0.0929-0.9532i -0.3260+02854i -0.3260-02854i -0.0265	-0.2617+0.0583i -0.2617-0.0583i -03466+03369i -03466-03369i -0.0226
-0.0550+09692i -0 0550-09692i -03673+03841i -03673-03841i -0.0198	-0.354+09813i -0.354-09813i -03880+04273i -03880-04273i -0.0177	-0.0161+0.9964i -0.0161-0.9964i -0.4080+0.4668i -0.0161	**Table 10** **ALPHA = 170 degrees** **SLIP = 0-01:1.0**

The Routh's stability criterion tells us whether or not there are unstable roots in a polynomial equation just as it is state ' in [8, 9]. To confirm the stability state by this approach, the polar plots of the roots for a firing angle of 120 degrees with slip range from zero to one are presented in figures (2) to (12) that follow.

POLAR PLOTS OF THE ROOTS ON THE PLANE,

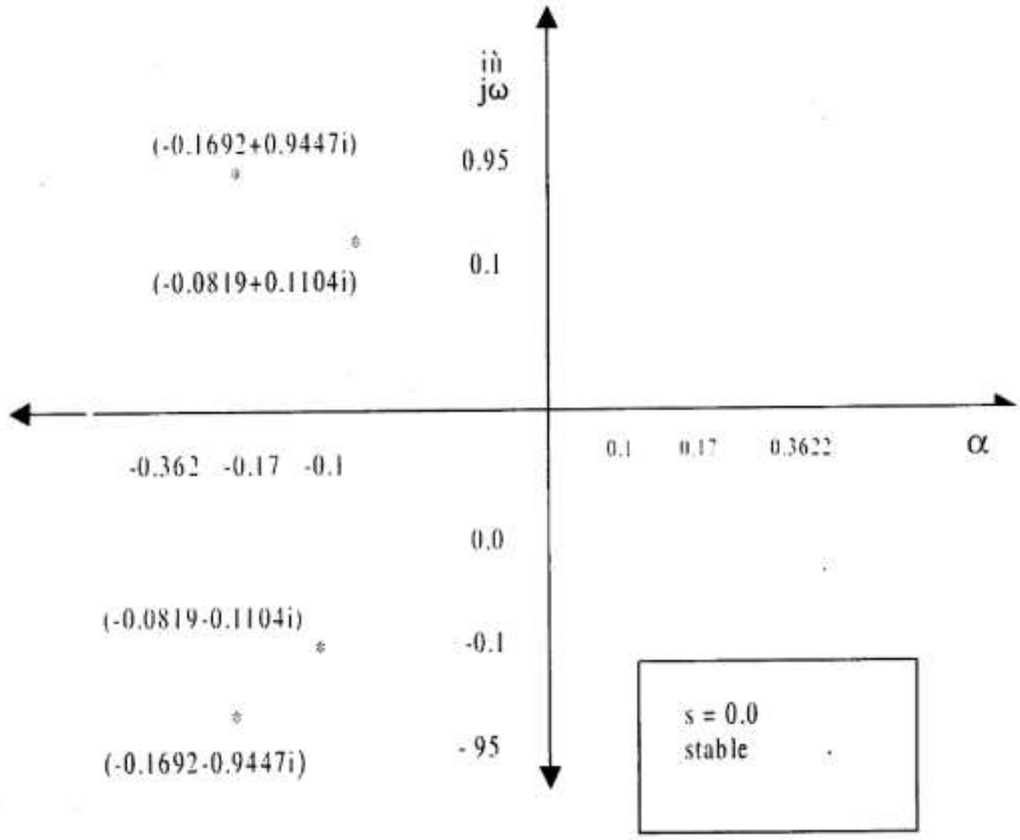

Fig. 1: Polar plot for slip 0 = 0.

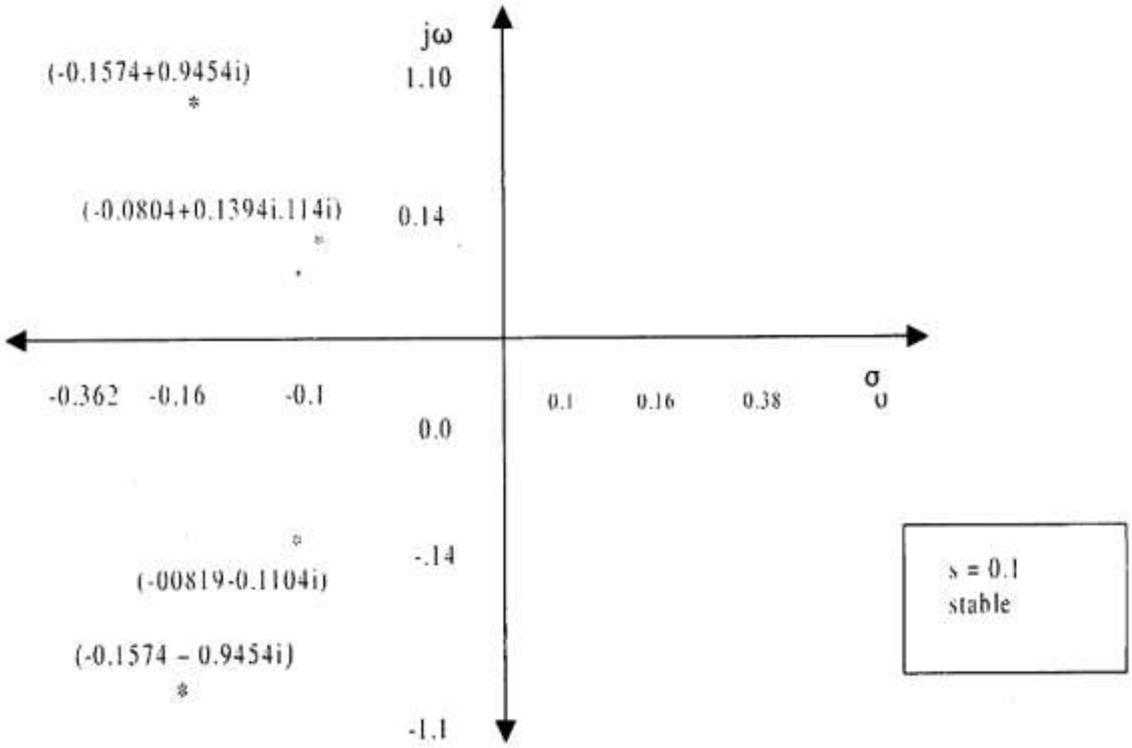

Fig. 2: Polar plot for slip = 0.1.

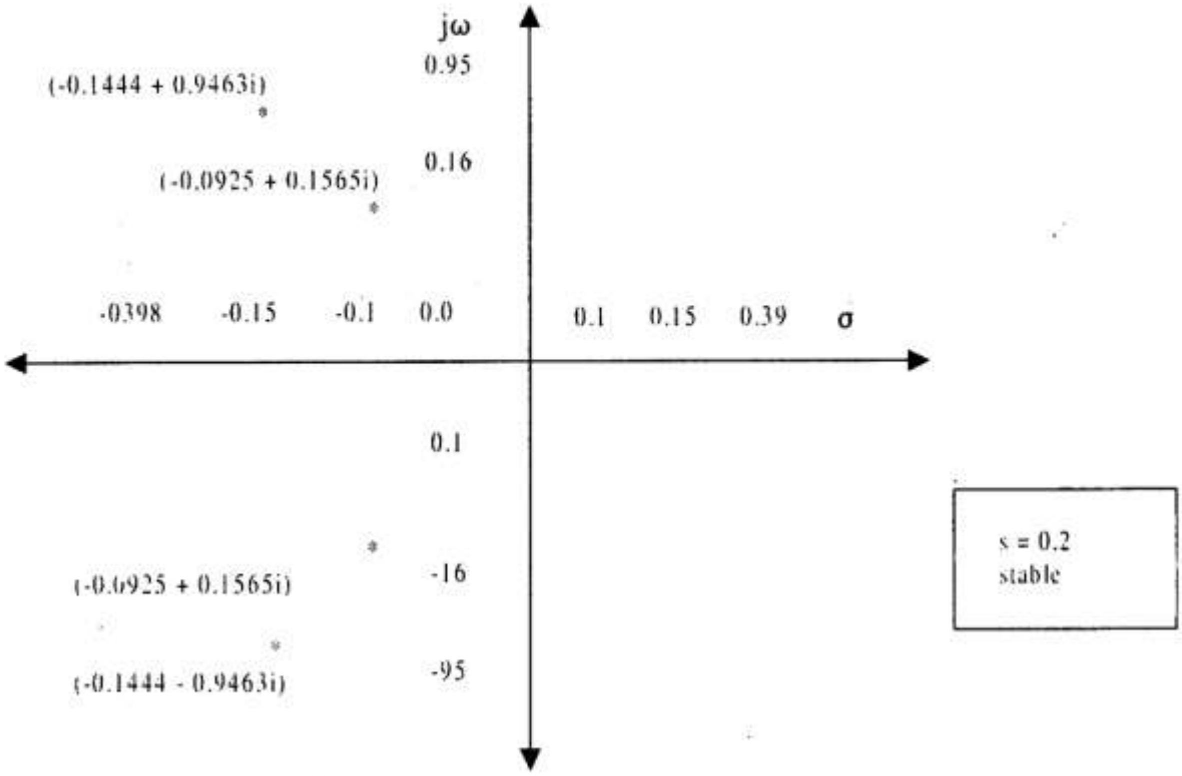

Fig. 3: Polar plot for slip = 0.2.

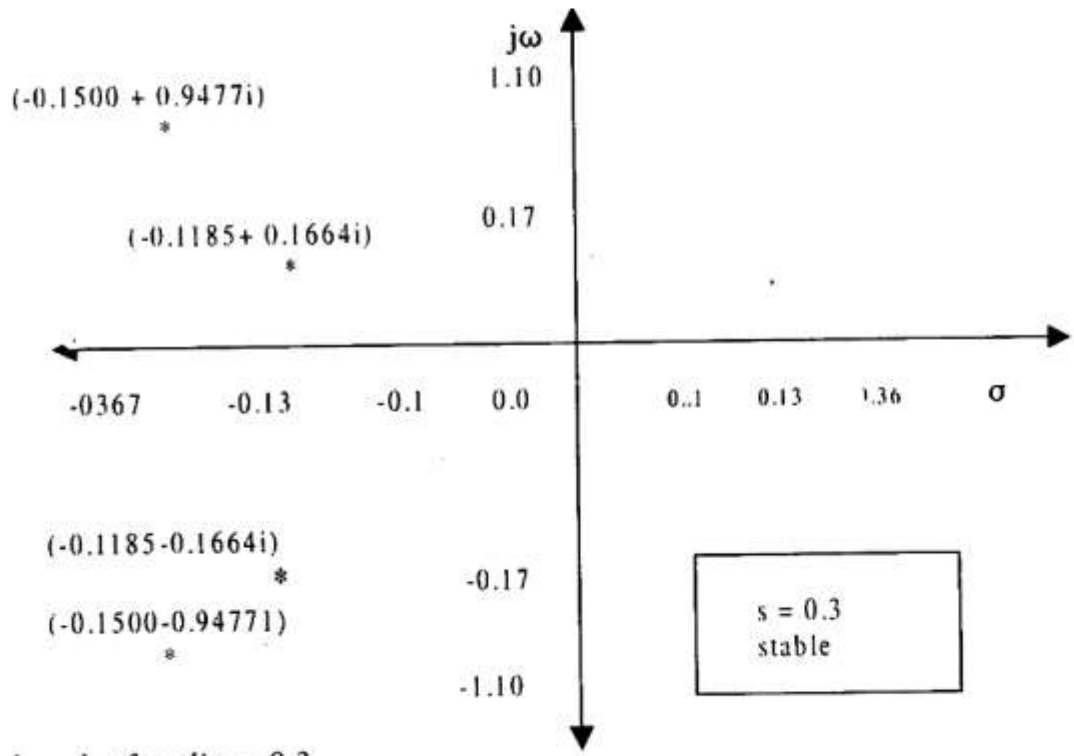

Fig. 4: Polar plot for slip = 0.3.

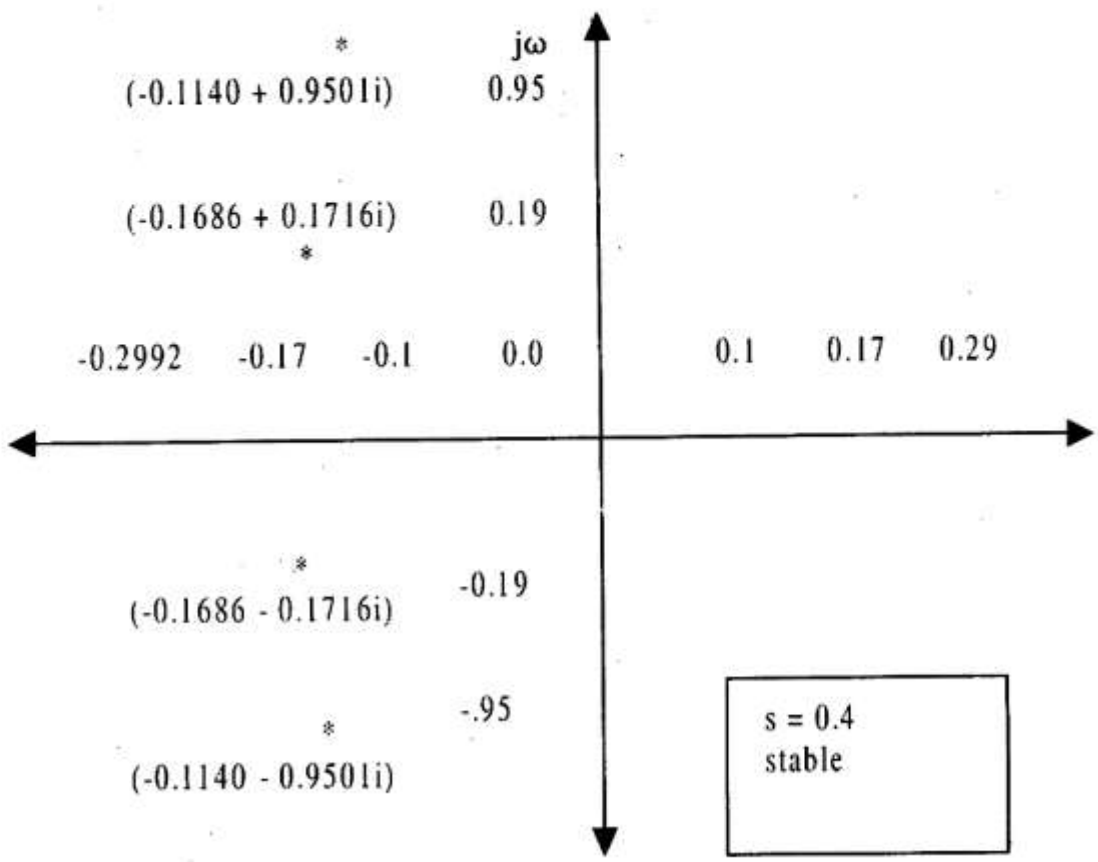

Fig. 5: Polar plot for slip = 0.4.

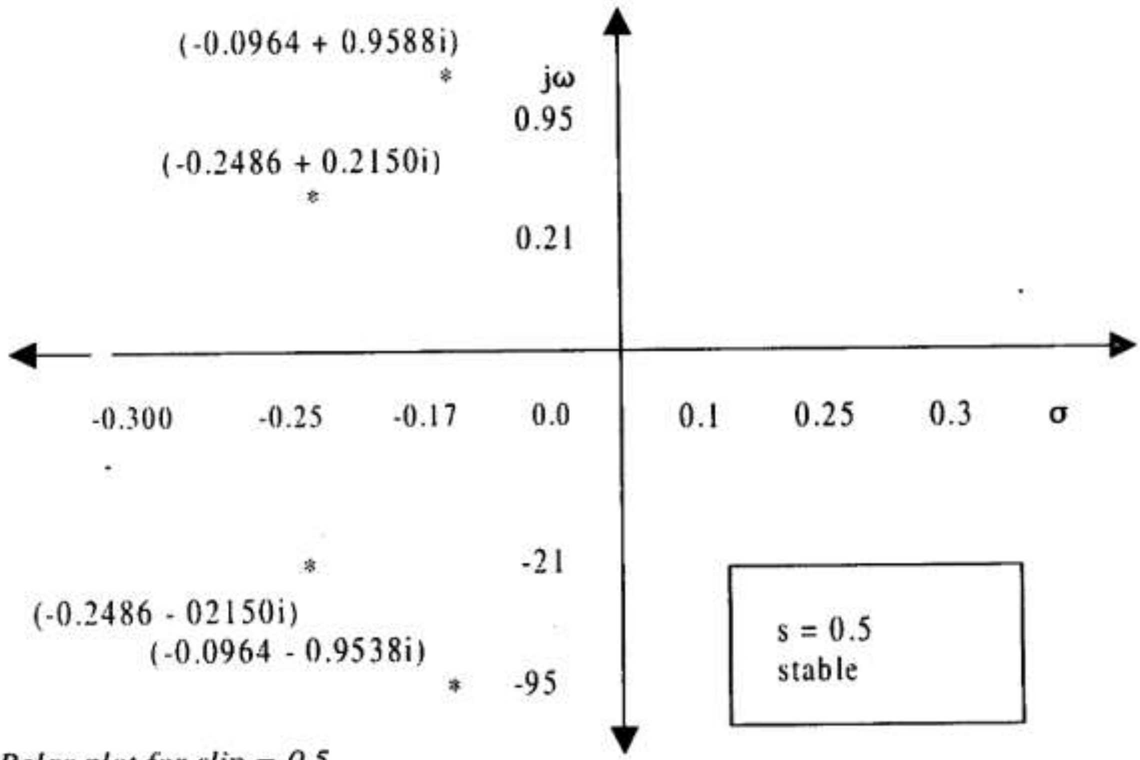

Fig. 6: Polar plot for slip = 0.5.

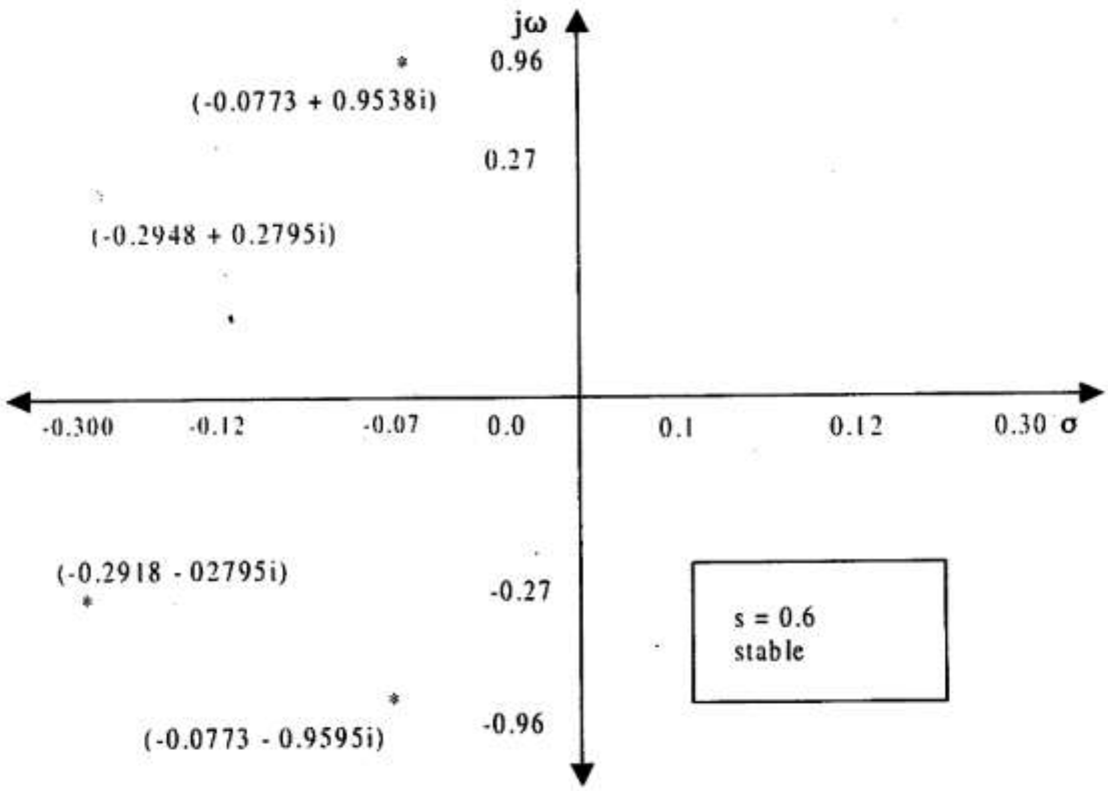

Fig. 7: Polar plot for slip = 0.6.

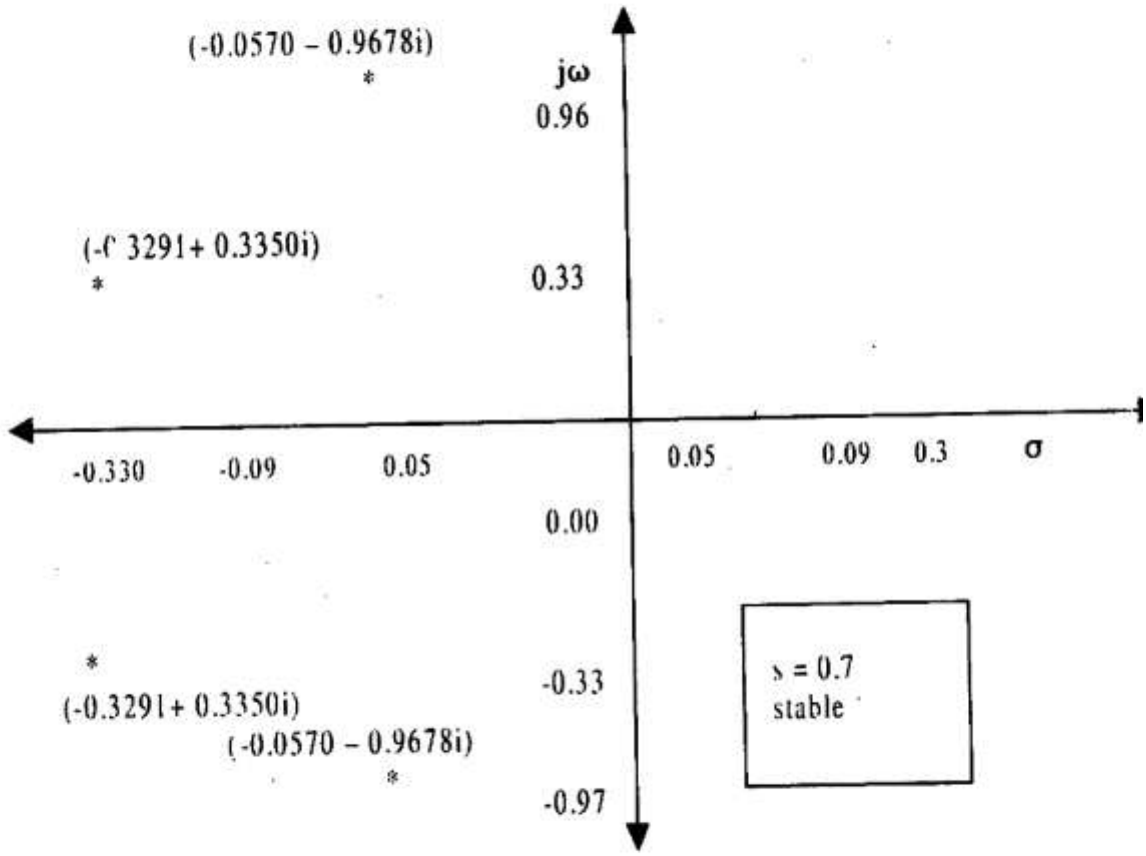

Fig. 8: Polar plot for slip = 0.7

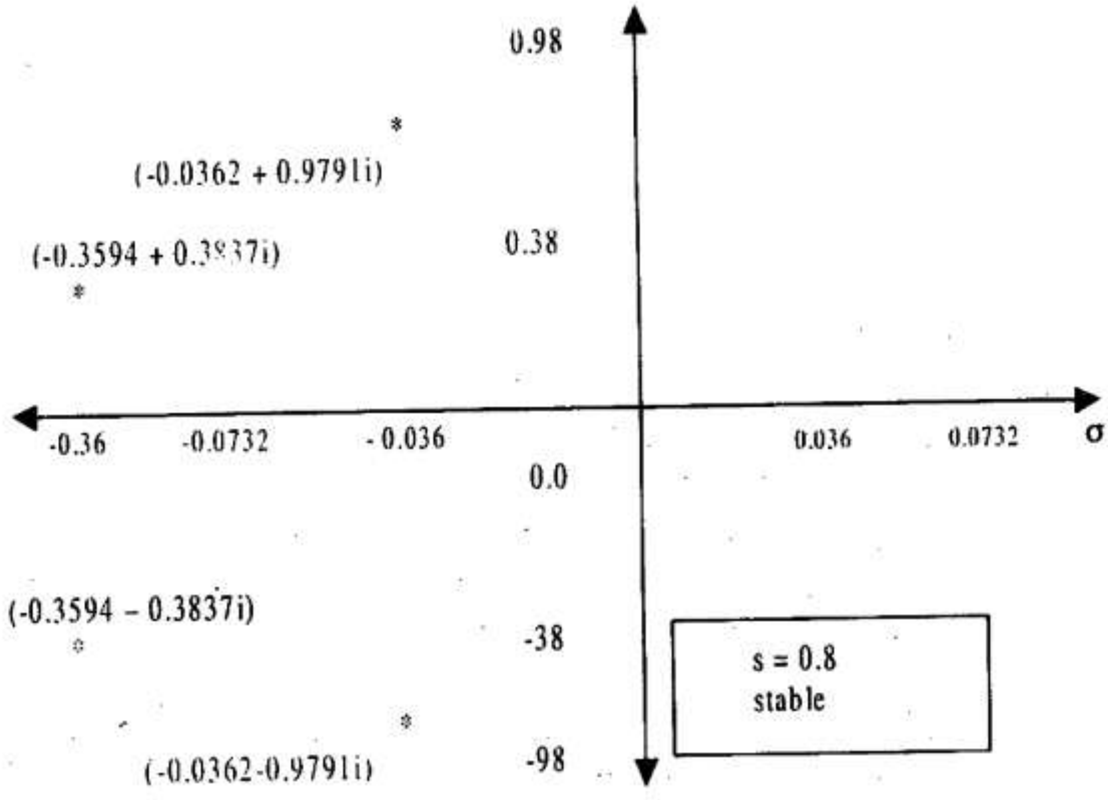

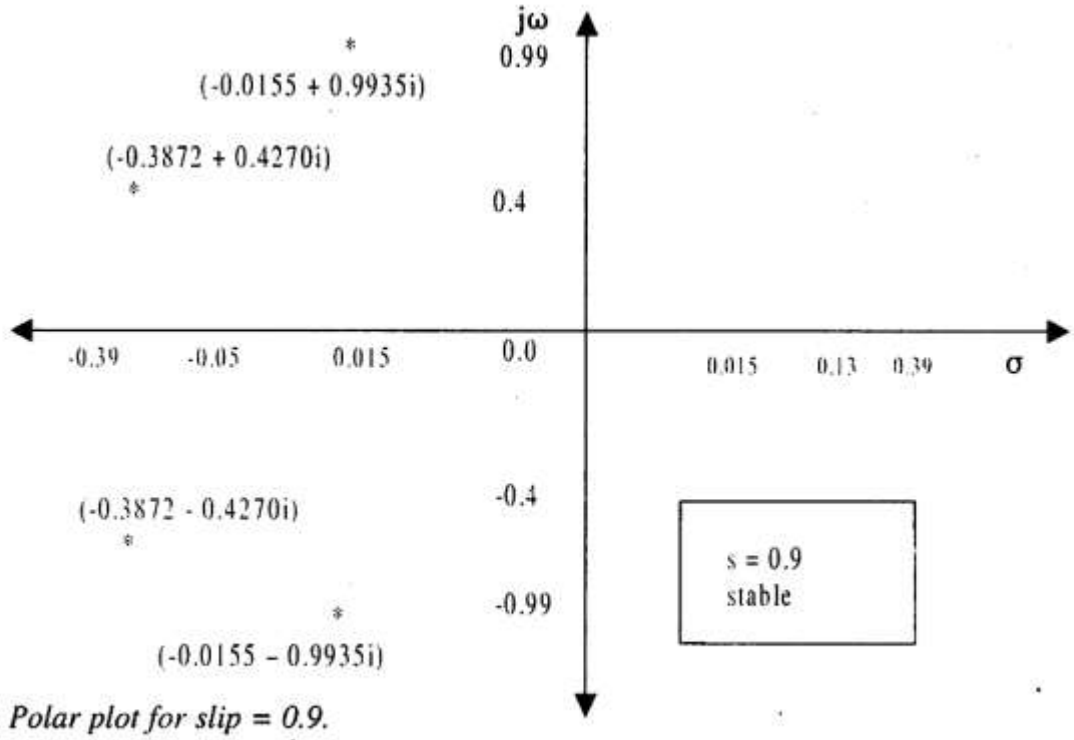

Fig. 10: Polar plot for slip = 0.9.

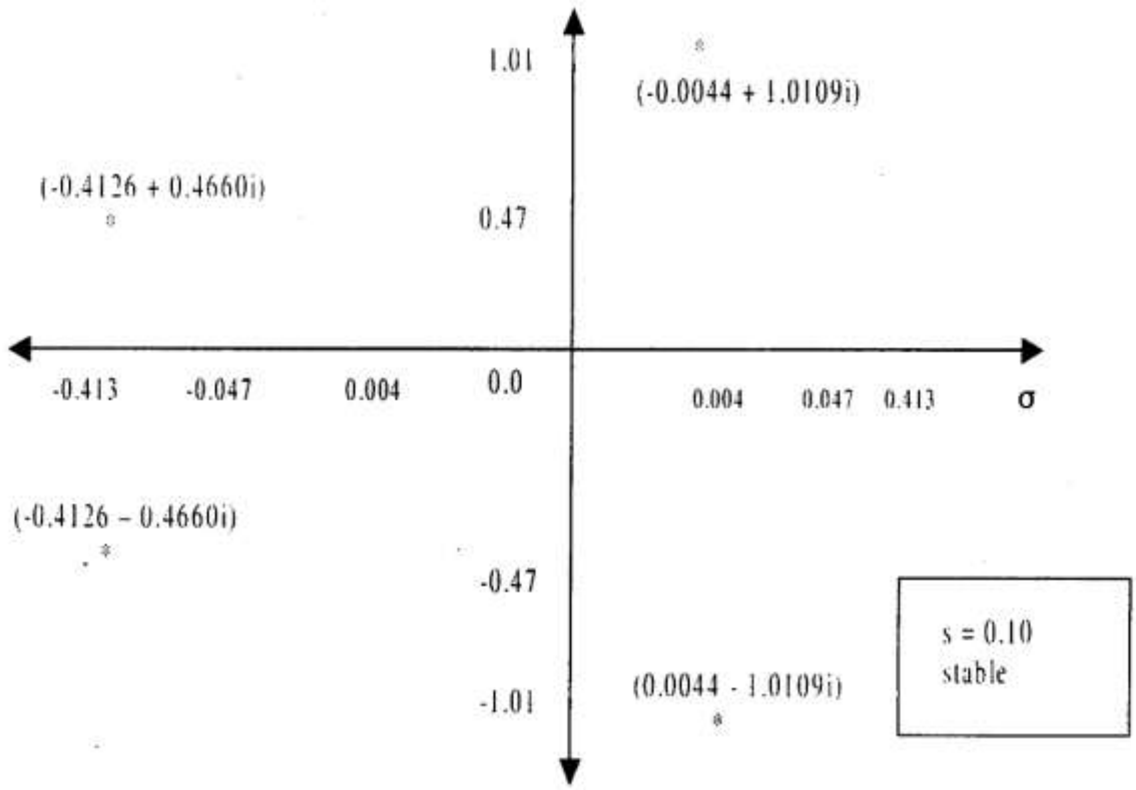

Fig. 11: Polar plot for slip = 1.0.

5.0 CONCLUSION

The need to have a unified theory as against the contradicting theories existing on the stability of induction machine with a static sub synchronous convertor cascade in the rotor circuit led to the timely and in-depth study of this work. The Eigenvalues analysis of the linearized model of an induction motor by the small signal perturbation method shows that the system in general terms does not become unstable. A confirmation of the system stability from Routh's stability criterion shows that the points lie on the left hand side of the plane.

Finally, as far as the normal operating region of the system is concerned, instability does not exist especially as the firing angle is increased, hence the slip energy recovery drive from the point of view of stability is superior to variable-frequency induction motor drives and as such, its application is highly recommended for fans, blowers and pumps.

In practice, the exact drive as modeled here cannot be realized owing to the effects of non-linearities and assumptions. However, the elegance of this drive scheme is in the fact that its control signal (current controller) is limited so as to limit the firing angle to its upper limit of maximum firing angle. Another significant point is that unlike the phase controlled induction machine where the three phase currents are involved, here the sensing of only one current, d c link current is sufficient for feedback control. This simplifies the control scheme compared to other ac drive schemes.

REFERENCES

[1] Murray L. Macdonald and Paresh C. sen,'Control loop study of induction motor drives using D-Q model', *IEEE Transaction on industrial electronics and control instrumentation*, vol. 26, No.4, Nov.1979, pp. 237-241.

[2] V.N. Mittle, K. Venkatesan and S.Gupta,'Stability analysis of a constant torques static slip-power-recovery drive, *IEEE Transactions on industry applications*, vol. IA 16, No.1, January /February 12980, pp.119 126.

[3] V.subrahmanyam, K. Surendran, ‘On the stability of a static slip energy recovery drive’, *IEEE Proceedings*, vo1.134, part B No.6, November 1987, pp.364-368.

[4] R. Krishman. 'Electric motor drives, Modeling *analysis and control'*, Prentice-Hall inc, New Jersey, 2001.

[5] Paul C. Krause, *'Analysis of Electric machinery;* Mc Graw-Hill Book Inc. U.S.A., 1986.

[6] Ogbonnaya.I. Okoro. *'Introduction to Matlab/Simulink for Engineers and Scientist,'* John Jacob's Publishers Ltd. Enugu, March, 2005.

[7] Katshuhiko Ogata, *'Modern Control Engineering,'* Prentice Hall India, New Delhi, 1991.

[8] Charles K. Alexander, Mathew N.O. Sadiku, '*Fundamentals of Electrical Circuits*', McGraw· Hill inc. U.s.A., 2000

[9] Chi-Tsong Chen, *Linear system theory*

and design', Holt-Saunders International editions, Japan, 1984.

1. APPENDIX

A List of tables

Table 1: Simulation parameters
Table 2: Eigenvalues for Alpha =90 degrees
Table 3: Eigenvalues for Alpha = 100 degrees
Table 4; Eigenvalues for Alpha =110 degrees
Table 5: Eigenvalues for Alpha =120 degrees
Table 6: Eigenvalues for Alpha =130 degrees
Table 7: Eigenvalues for Alpha =140 degrees
Table 8: Eigenvalues for Alpha =150 degrees
Table 9: Eigenvalues for Alpha =160 degrees
Table 10: Eigenvalues for Alpha = 170 degrees

B List of figures

Figure 1: Polar plot for slip = 0.0
Figure 2: Polar plot for slip = 0.1
Figure 3: Polar plot for slip = 0.2
Figure 4: Polar plot for slip = 0.3
Figure 5: Polar plot for slip = 0.4
Figure 6: Polar plot for slip = 0.5
Figure 7: Polar plot for slip = 0.6
Figure 8: Polar plot for slip = 0.7
Figure 9: Polar plot for slip = 0.8
Figure 10: Polar plot for slip = 0.9
Figure 11: Polar plot for slip = 1.0